1

Heat and Mass Transfer

1.1 Introduction

Commercial grade raw material calcination in a rotary kiln is common to make an economical product. The end product feeding regions are divided into several segments to achieve calcined outcomes like dolomite, spinel, mag-chrome, bauxite, etc. Ineffective heat distribution and mass-transfer during rotation result in an immature and uncalcined product that eventually reduces the properties of the refractories. While considering the nonuniform heat distribution in a kiln, there is always a chance to form a premature uncalcined product with a moisture-absorbing tendency; dolomite is an excellent example. Similarly, incomplete spinel conversion from a mixture of MgO and Al_2O_3 in synthetic raw materials eventually enhances the volume expansion in spinel-based refractory, as well as the improper calcination of natural bauxite facilitates forming a porous mass that absorbs more water during the castable casting results in premature failure.

Organic binder essentially develops a polymeric network and binding refractory grains, but a gradual formation of ceramic bonding requires a predefined temperature in the firing. Tunnel or batch kilns are used in the refractory industry to achieve prerequisite temperatures for high-performance working lining, backup lining, and continuous casting refractories. A highly efficient kiln may provide uniform heat distribution all along the sides from top to bottom, sidewall burner zone to opposite side wall burner zone, car to car, and brick stack to stack; otherwise, some bricks are overfired or underfired. Low temperature is responsible for higher porosity, low bulk density, and cold crushing strength. In contrast, overfired may produce unexpected expansion/shrinkage behavior and low eutectic phases in the presence of impurities.

Precast and Refractory lining preheating in the steel industry shop floor is essential before processing molten steel. Process efficiency depends on the refractory material properties like density, thermal conductivity, and specific heat. However, the foremost thing is the employed process temperature and how

Fundamental Design of Steelmaking Refractories, First Edition. Debasish Sarkar.

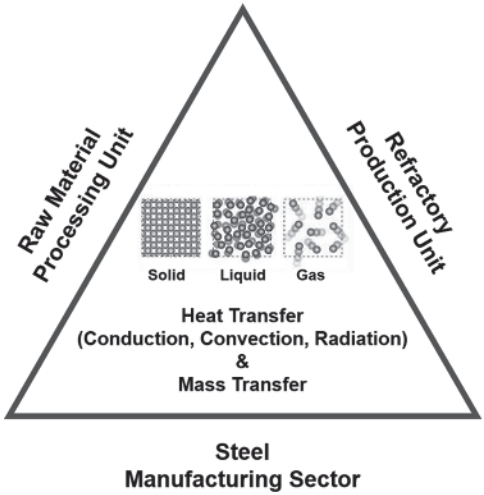

Figure 1.1 A schematic representation of heat and mass-transfer in refractory processing, production, and application sectors. The atomic arrangement defines solid, liquid, and gas states and possible separation under heat.

it is transferred effectively throughout the system. Continuous argon gas purging through a porous plug facilitates homogenous molten steel composition and temperature throughout the vessel. This multiphase heat transfer behavior differs from heat transfer in a single-phase solid or gaseous environment. Moreover, there is enough scope for heat loss from steel vessels (BOF, LF, Tundish) either through the open space or refractory lining. Different refractory quality experience a temperature gradient due to differences in thermal conductivity from working to safety lining in a vessel.

Raw material calcination, shaped refractory firing, refractory preheating, maintaining uniform temperature in the entire mass of molten steel, and temperature loss through working lining to the outer vessel shell are critical issues and worthy of analyzing the perspective of heat and mass-transfer phenomena. A schematic representation of such a relation is given in Figure 1.1. The inset solid to liquid to gas conversion depends on the temperature that usually enhances kinetic energy and diffusion of atoms. Thus, heat and mass-transfer fundamentals are considered a starting discussion to explore the properties and analysis for the designing refractory for the steel sector.

1.2 Energy Conservation

Industry measures the temperature profile in a kiln or furnace, but heat distribution is technically responsible for device efficiency. The temperature is different from the heat. The heat transfer is distinctly different from thermodynamics.

Temperature (T, °C) measures the quantity of energy influenced by the molecules of a material or system and predicts both the degrees of hotness and direction of heat transfer. Heat (Q, Joule) measures thermal energy transfer from a hotter body to a colder one. Thus, heat transfer describes how much heat, transfer rate, and resultant temperature distribution are inside the body. However, thermodynamics is concerned with the equilibrium state of matter, the amount of heat transferred (dQ), the amount of work done (dW), and the final form of the system. In practice, heat transfer is complementary and an extension of thermodynamics.

a) Control Volume (Open system)

The first law of thermodynamics defines the conservation of total energy and can only change if it crosses the boundaries. A region of fixed mass known as the closed system allows the transfer of heat through boundaries and work done on or by the system, resulting in the total energy changes of the system, as illustrated in Equation (1.1) and Figure 1.2a.

$$\Delta E_{\text{system}} = Q - W \tag{1.1}$$

Where total energy change stored in the system is ΔE_{system}, net heat transferred to the system is Q, and new work done by the system is W. In the same chronology, control volume (or open system) region has many possible mass entries. Herein, the "many" terminology refers to the possibility of the energy it carries with it when entering and leaving the mass in the control volume, known as energy advection, which facilitates energy across the boundaries of a control volume. Thus, energy can enter and leave the control volume due to heat transfer from the boundaries, work done on or by the control volume, and energy advection. The total energy combines internal energy and mechanical energy (cumulative potential and kinetic energy). Internal energy can be further subdivided by thermal energy and other forms of internal energy, such as chemical and nuclear energy. Thermal and mechanical forms of energy are a prime concern in heat transfer. The sum of these energies is not conserved because of the possibility of conversion between other forms of energy and thermal energy. However, the stored energy rate must be balanced during inflow and outflow energy in the control volume.

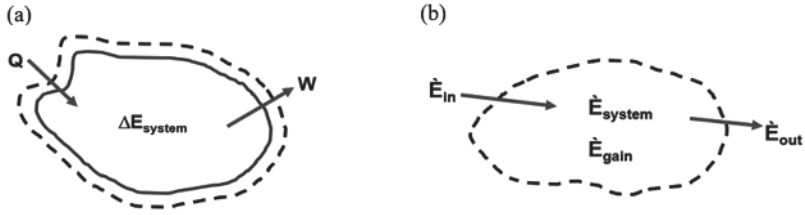

Figure 1.2 (a) Closed system with a time interval (Δt), (b) control volume instantly.

Thus, the change in mechanical and thermal energy stored (ΔE_{stored}) over the time interval Δt and generation of thermal energy (E_g) in the control volume is:

$$\Delta E_{stored} = E_{in} - E_{out} + E_g \tag{1.2}$$

The incidence rate of stored energy ($\dot{E}_{stored}$) increment in the controlled volume is represented in Figure 1.2b and calculated by Equation (1.3):

$$\dot{E}_{stored} = \frac{dE_{stored}}{dt} = \dot{E}_{in} - \dot{E}_{out} + \dot{E}_g \tag{1.3}$$

Total mechanical energy represents the sum of KE (kinetic energy $= \frac{1}{2}mv^2$, where m is the mass and v is the velocity, respectively); PE (potential energy $= mgh$, where g and h are the gravitational acceleration and vertical distance, respectively); and U (internal energy). However, the internal energy (U) consists of:

i) A *sensible* component comprised of rotational, translational, and vibrational motion of the molecules/atoms of the matter;
ii) Component of *latent* indicates the intermolecular forces influencing the changes in phase between vapor, liquid, and solid states;
iii) Accounts of *chemical* components for stored energy in the chemical bonds in atoms; and
iv) The accounts of *nuclear* components for the binding forces in the nucleus.

In a heat transfer study, sensible (U_{sen}) and latent (U_{lat}) are the most important internal energy components and together are known as thermal energy (U_t); thus, $U_t = U_{sen} + U_{lat}$. Sensible and latent energy is responsible for temperature (although it depends on pressure) and phase change, respectively. For example, in the control volume region, if the material changes from solid to liquid represents melting, and liquid to vapor indicates vaporization, boiling, and evaporation, the latent energy increases. Conversely, condensation (vapor to solid) or solidification and freezing (liquid to solid) decreases the latent energy. Thus, stored energy (E_{stored}) is, $E_{stored} = KE + PE + U_{sen} + U_{lat}$. The KE and PE are often small, and if there is no phase change, both mechanical energy and U_{lat} can be neglected, and thus, $E_{stored} = U_{sen}$; if no temperature change, $E_{stored} = U_{lat}$.

The inflow and outflow incidence in the control volume region is initiated from a surface; thus, it is a surface phenomenon. The process exclusively on the control surface is ordinarily proportional to the surface area. Therefore, the concepts of inflow and outflow of energy terms include the transfer of heat associated with solid medium (conduction), liquid presence (convection), vacuum (radiation), and work interactions that occur at the boundaries of the system. If mass enter or leave the control volume boundary, both the inflow and outflow advected mechanical and thermal energy in the control volume. For instance, if entering mass-flow rate $\dot{m}$, then the control volume is the product of $\dot{m}$ ($u_t + ½v^2 + gh$),

where u_t represents the thermal energy per unit mass, and ($½v^2 + gh$) is the mechanical energy per unit mass.

b) Surface Energy Balance

Energy conservation at the surface is an important aspect. As shown in Figure 1.3, the control surfaces are assumed on either side of the bold physical boundary where no mass or volume is enclosed. Herein, Equation (1.3) is no longer valid and only deals with surface phenomena considering the energy storage and generation concept. Under this circumstance, the conservation becomes:

$$\dot{E}_{in} - \dot{E}_{out} = 0 \tag{1.4}$$

Although thermal energy generation may occur in the medium, the control surface energy balance is not affected and holds steady-state and transient conditions. On the unit area basis, three heat transfer terms are shown for the control surface in Figure 1.3.

Under this circumstance, the conduction is in between medium and control surface (q''_{cond}), the surface to a fluid (q''_{conv}) indicates convection, and exchange of the net radiation between the surface to the surroundings (q''_{rad}) can be balanced by Equation (1.5). In brief, the heat flux (q/A, q = heat rate, A = area) for conduction, the $q''_{cond} = k\,(\Delta T/L)$:

$$q''_{cond} - q''_{conv} - q''_{rad} = 0 \tag{1.5}$$

where k = thermal conductivity (W/m.K), ΔT, and L are temperature differences and thickness of the medium, respectively.

In convection, $q''_{conv} = h\,(T_s - T_\infty)$, where h = heat transfer coefficient (W/m^2.K), T_s is surface temperature, and T_∞ is fluid temperature. In radiation, $q''_{conv} = \varepsilon\sigma(T^4_s - T^4_{sur})$, where ε is emissivity ($0 \le \varepsilon \le 1$), σ = Stefan–Boltzmann constant ($\sigma = 5.67 \times 10^{-8}$ W/m^2.K^4), T_{sur} is the surrounding temperature. From

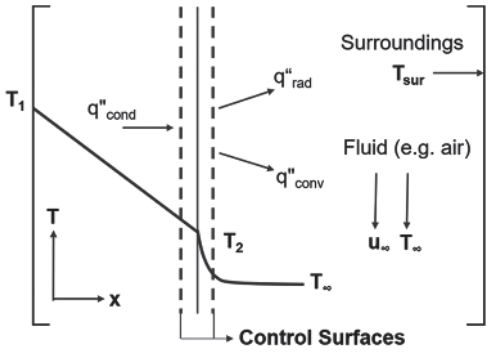

Figure 1.3 The energy balance for energy conservation at the surface of a medium.

a thermodynamic perspective, it is reasonably clear why conduction, convection, and radiation are important aspects to explain heat transfer mechanisms and energy balance. Thus, the origin and details of each mechanism are explained in the next section.

1.3 Conduction

High temperature aggravates molecular energies, and collision facilitates energy transfer to adjacent low energy molecules. This incidence develops thermal gradient and heat flow from higher to lower temperature regimes in the conduction process. Despite a collision, the random motion of molecules is also responsible for energy transfer, but a collision accelerates the energy transfer rate. This class of net energy transfer is nothing but the diffusion of energy. Eventually, the heat transfer by conduction relies on direct contact between atoms or molecules that can also be materialized in gas and liquid, not only in solid. Molecules are more closely packed in liquids than gas, and their interactions are more frequent and substantial. Similarly, conduction attributes to atomic activity in the translational motion of free *e* in a solid.

1.3.1 Basic Concept and Properties

In consideration of Fourier's law, high school science describes simple steady-state conductive heat flow relation by heat flux, thermal gradient, and thermal conductivity of materials. Consider a steel cylinder insulated on its lateral surface, as illustrated in Figure 1.4. The heat flow occurs from one end to another when end faces have different temperatures, say T_1 and T_2, where $T_1 > T_2$ follows the one-direction flow, and x represents direction only.

The temperature difference induces heat transfer. The rate of heat transfer (q_x) depends on the variables ΔT—temperature difference, Δx—cylinder length, A—area of cross-section, and can be represented by Equation (1.6).

$$q_x \propto A\frac{\Delta T}{\Delta x} \tag{1.6}$$

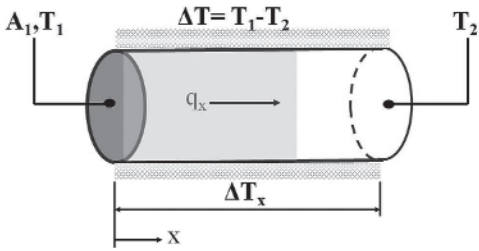

Figure 1.4 Schematic representation of steady-state heat conduction experiment.

This heat transfer rate becomes lower for alumina (Al_2O_3), and lowest for high-density polyethylene (HDPE) compared to equal A, Δx, and ΔT of the steel cylinder. Thus, this proportionality converts into a coefficient, k, known as thermal conductivity (W/m.K) and Equation 1.6 to be:

$$q_x = kA\frac{\Delta T}{\Delta x} \tag{1.7}$$

Consider Figure 1.5a, and solving Equation 1.7, when $\Delta x \to 0$, the heat rate Equation 1.7 becomes Equation 1.8, in which the negative sign is mandatory because the flow of heat is always in the temperature decreasing direction; thus, temperature gradient dT/dx is −ve, and q''_x is +ve.

$$q_x = -kA\frac{dT}{dx} \tag{1.8}$$

Or the isothermal surfaces are planes normal to the x-direction, and the heat flux:

$$q''_x = \frac{q_x}{A} = -k\frac{dT}{dx} \tag{1.9}$$

Heat flux is a vector quantity, and a general statement of Fourier's law of conduction follows Equation (1.10), where T(x,y,z) is the scalar temperature field:

$$q'' = -k\left(i\frac{\partial T}{\partial x} + j\frac{\partial T}{\partial y} + k\frac{\partial T}{\partial z}\right) \tag{1.10}$$

In more generalized terms this equation can be written as:

$$q''_n = -k\frac{\partial T}{\partial n} \tag{1.11}$$

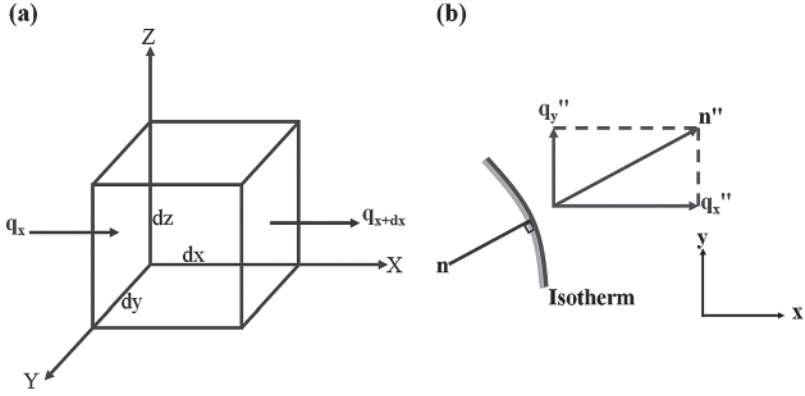

Figure 1.5 (a) Heat flow along x-direction in a cubic system, (b) heat flux vector for a two-dimensional system.

Where, q''_n is the heat flux in n direction, normal to an isotherm for two coordinate systems, as shown in Figure 1.5b. Table 1.1 provides the probable thermodynamic data for the materials associated with refractory analysis. Detailed fundamental concepts of thermal conductivity and the effect of temperature on conductivity variation are discussed in Chapter 5, Section 5.4.

Heat transfer analysis requires many thermophysical properties, including two distinct groups, thermodynamic and transport properties of a matter. The transport properties have the diffusion rate coefficients such as thermal conductivity (k) for the heat transfer and kinematic viscosity (ν), for momentum transfer. In other words, the density (ρ) and specific heat (c_ρ) refer to the thermodynamic properties. Product ρc_ρ (J/m^3.K), known as volumetric heat capacity, is essential for measuring thermal energy storage ability. High-density materials have low

Table 1.1 Thermal properties of different materials.

	K (W/m.K)			
Material	**100°C**	**1000°C**	**ρ(g/cc)**	**c_ρ(J/kg.K)**
SiO_2	2	2.5	2.65	732
Fe_2O_3	8.5	2.38	5.25	104
TiO_2	6.7	3.35	4.25	690
MnO	1.3	1.24	5.43	611
CaO	15.48	7.84	3.32	418
MgO	38	7.1	3.58	890
Cr_2O_3	32	10	5.23	529
B_4C	30	42	2.51	1000
Steel	13.2	30.8	7.86	502
Al_2O_3	30	6.3	3.99	160
ZrO_2	1.9	2.3	6.09	450
SiC	370	30	3.22	344
Graphite	179.9	62.7	2.27	711
Al_4C_3	107.8	98	2.97	–
Si_3N_4	19.66	15.90	3.19	712
H_2O	0.025	0.121	1	4184
O_2	0.032	0.036	0.00143	917
CO_2	0.023	0.072	1.56	709
Ar	0.019	0.058	1.784	519

specific heat, act as a perfect energy storage media, and have value in $\rho c_\rho > 1$ MJ/m^3·K. In contrast, gases are low-grade energy storage media in the range of $\rho c_\rho \approx 1$ kJ/m^3·K. With the help of thermal conductivity, density, and specific heat, the thermal diffusivity $\alpha = k/(\rho c_\rho)$ implies the ability to conduct thermal energy relative to its ability to store thermal energy, an essential phenomenon during sintering. High diffusivity refers to rapid change in their thermal environment to maintain equilibrium. Selecting reliable data for a particular phase is critical to drawing a convincing conclusion during heat transfer analysis.

1.3.2 One-Dimensional Steady-state Conduction

Heat transfer by diffusion is directly proportional to the temperature gradient (except thermal radiation), and it is expected that heat flux transportation will vary in one-dimensional (x), two-dimensional (x,y), and three-dimensional (x,y,z). The majority of the heat transfer occurs in one-dimension: heat transfer from the inner wall to the outside of a kiln when two sides maintain a temperature gradient. Two-dimensional heat transfer is a vital function of the corresponding cross-section without variation of the third dimension. Fins extended surfaces are used for heat transfer between a hot body and its surroundings, an excellent example of two-dimensional flow. However, in many cases, the one coordinate direction heat flow is oversimplified and necessary to account for multidirectional effects.

Where one-dimension steady-state conduction is concerned, two types of heat transfer phenomena may be observed, "without internal heat generation (heat dissipation through a refractory wall)" and "with internal heat generation (during energy conversion from electrical or chemical to thermal energy)." Refractory lining for a tunnel kiln is an excellent example of the heat transfer process with no heat generation possible through a plane wall. However, contact resistance may appear during such transfer because of different phases (e.g., air) within composite layers. In Figure 1.6a, two fluids are separated by a single plane wall at different temperatures. Heat transfer from the hot fluid at $T_{\infty 1}$ to the inner wall surface by convection at T_{s1}, by conduction through the wall, and further outer wall surface at T_{s2} to the cold fluid at $T_{\infty 2}$ through the convention.

For one-dimensional *(→x)*, steady-state conduction in a plane wall with no heat generation and constant thermal conductivity (k), the temperature varies linearly with x. Thus, the conduction heat transfer rate (from Equation 1.8) is:

$$q_x = -kA\frac{dT}{dx} = \frac{kA}{L}(T_{s1} - T_{s2}) \tag{1.12}$$

Herein, the prescribed surface temperatures at $x = 0$ and $x = L$ are boundary conditions, although this temperature strictly depends on the homogeneity of fluid temperature. Analogous to electrical resistance, the thermal resistance for

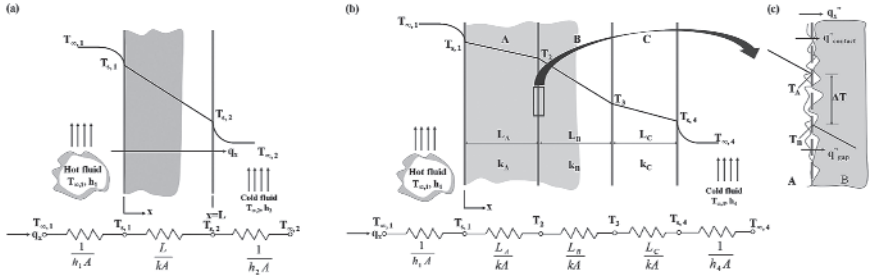

Figure 1.6 Heat transfer through (a) a plane wall, (b) equivalent thermal circuit for a series composite wall (example of kiln lining), (c) temperature drop due to thermal contact resistance.

conduction in a plane wall is associated with thermal conductivity and can be written as:

$$R_{t,cond} = \frac{\left(T_{s1} - T_{s2}\right)}{q_x} = \frac{L}{kA} \tag{1.13}$$

Thermal conductivity (k) of insulating solid depends on heat capacity per unit volume (C), average phonon velocity (v), and mean free path (l). The C is reduced by the system's porosity volume fraction (p), and the resultant k becomes; where C^{o} is the heat capacity at $p = 0$. Thus, k can be represented as Equation (1.14):

$$k = \frac{1}{3} vlC_o(1-p) \tag{1.14}$$

From Equation (1.14), it is obvious why porous ceramics are preferred as insulating surfaces to reduce heat loss from the kiln's outer wall. Thermal resistance is often associated with heat transfer through convection to a surface and conductive resistance. According to Newton's law of cooling, the heat rate q may be represented by Equation (1.15), where h is the heat transfer coefficient in convection:

$$q_x = hA(T_s - T_\infty) \tag{1.15}$$

The thermal resistance for convection is:

$$R_{t,conv} = \frac{\left(T_s - T_\infty\right)}{q} = \frac{1}{hA} \tag{1.16}$$

The heat transfer rate is constant throughout the system; thus q_x becomes:

$$q_x = \frac{\left(T_{\infty 1} - T_{s1}\right)}{\frac{1}{h_1 A}} = \frac{\left(T_{s1} - T_{s2}\right)}{\frac{L}{kA}} = \frac{\left(T_{s2} - T_{\infty 2}\right)}{\frac{1}{h_2 A}} \tag{1.17}$$

In consideration of overall temperature difference $T_{\infty 1} - T_{\infty 2}$, and the total thermal resistance R_{tot}, the heat transfer rate may be written as:

$$q_x = \frac{\left(T_{\infty 1} - T_{\infty 2}\right)}{R_{tot}} \tag{1.18}$$

Where R_{tot}:

$$R_{tot} = \frac{1}{h_1 A} + \frac{L}{kA} + \frac{1}{h_2 A} \tag{1.19}$$

Exchange of radiation between surface and surroundings may also be important when h for convection is very small. The thermal resistance for radiation $R_{t,rad} = (T_s - T_{sur})/q_{rad} = 1/(h_r A)$, where h_r:

$$h_r \equiv \varepsilon\sigma(T_s + T_{sur})(T_s^2 + T_{sur}^2) \tag{1.20}$$

Radiation of surface and resistances due to convection act parallel and can be combined to obtain a single, significant surface resistance if $T_\infty = T_{sur}$. In the exact chronology, the heat transfer rate (q_x) and overall heat transfer coefficient (U) may also be estimated for composite walls placed in a series connection, as shown in Figure 1.6b. The rate of heat transfer is:

$$q_x = \frac{\left(T_{\infty 1} - T_{\infty 4}\right)}{\frac{1}{h_1 A} + \frac{L_A}{k_A A} + \frac{L_B}{k_B A} + \frac{L_C}{k_C A} + \frac{1}{h_4 A}} \equiv UA\Delta T \tag{1.21}$$

Where

$$U = \frac{1}{R_{tot} A} = \frac{1}{\frac{1}{h_1 A} + \frac{L_A}{k_A A} + \frac{L_B}{k_B A} + \frac{L_C}{k_C A} + \frac{1}{h_4 A}} \tag{1.22}$$

The above equation is valid when heat flow presumed that surfaces normal to the x direction are isothermal, but R_{tot} is different when surfaces parallel to the x direction and the assumed adiabatic system.

Another critical factor, gap influenced by surface roughness filled by air, between the composite system interface is temperature drop, as shown in Figure 1.6c. This temperature change is known as thermal contact resistance $R_{t,c}$. The resistance per unit area of the interface is:

$$R''_{t,c} = \frac{T_A - T_B}{q''_x} \tag{1.23}$$

Conductive heat transfer follows through relatively minute contact spots, whereas convection and radiation across the gaps result in two parallel resistances. The

contact resistance may also be reduced by increasing the thermal conductivity of entrapped fluid or maximizing the contact spots, nothing but R_a's reduction (a statistical roughness parameter) value.

The heat transfer rate and resistance behavior are different for a cylindrical rotary kiln, a circular cross-section, as shown in Figure 1.7a. Cylindrical and spherical systems experience radial direction heat transfer, and thus the same one-directional approach may be employed to determine the heat transfer behavior.

Employing Fourier's law in circular geometry analogous to the single plane wall, the conductive heat transfer rate through radial mode (q_r) is:

$$q_r = \frac{2\pi Lk\left(T_{s1} - T_{s2}\right)}{\ln\frac{r_2}{r_1}} \tag{1.24}$$

And the thermal resistance:

$$R_{t,cond} = \frac{\ln\frac{r_2}{r_1}}{2\pi Lk} \tag{1.25}$$

Similarly, the q_r and U may also be calculated for the composite wall from Figure 1.7b:

$$q_r = \frac{T_{\infty 1} - T_{\infty 4}}{\frac{1}{2\pi r_1 L h_1} + \frac{\ln\frac{r_2}{r_1}}{2\pi k_A L} + \frac{\ln\frac{r_3}{r_2}}{2\pi k_B L} + \frac{\ln\frac{r_4}{r_3}}{2\pi k_C L} + \frac{1}{2\pi r_4 L h_4}} = UA(T_{\infty 1} - T_{\infty 4}) \tag{1.26}$$

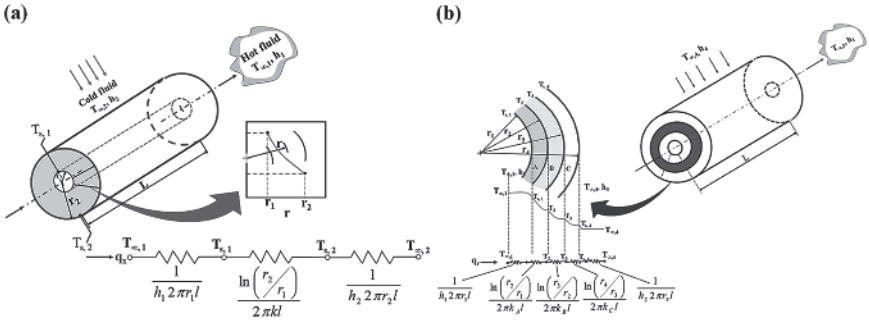

Figure 1.7 Heat transfer through (a) single hollow cylinder with convective surface conditions, (b) a composite cylindrical wall (an example of working, backup linings, and shell of a rotary kiln).

The overall coefficient may be defined as:

$$U_1A_1 = U_2A_2 = U_3A_3 = U_4A_4 = \left(\sum R_{tot}\right)^{-1} \tag{1.27}$$

An alternative integral approach can also estimate the one-dimensional heat transfer rate (q_x) for other shapes like conical systems (e.g., nose-tip of monoblock stopper). In consideration of:

Figure 1.8, any differential element dx, $q_x \rightarrow q_{x+dx}$, even if the area varies with position $A(x)$, and the thermal conductivity varies with temperature, $k(T)$. As the q_x is constant, we can express Fourier's law in the integral form:

$$q_x \int_{x_o}^{x} \frac{dx}{A(x)} = \int_{T_o}^{T} k(T)dT \tag{1.28}$$

In order to obtain the heat transfer rate for the nonuniform dimension, the cross-section area as a function of x (x_o to x) and change the thermal conductivity with temperature (T_o to T) is required. If area A is constant and thermal conductivity is independent of temperature, Equation (1.28) reduces to Equation (1.29):

$$\frac{q_x \Delta x}{A} = -k\Delta T \tag{1.29}$$

An alternative integral method effectively solves diffusion rate equations with a one-dimensional steady-state limiting condition with no heat generation. A simplified integral approach may estimate the heat transfer rate for the sphere (Figure 1.9). The appropriate form of Fourier's law for one-dimensional steady-state heat transfer rate for the sphere is Equation (1.30), where $A = 4\pi r^2$ is the area normal to the direction of heat transfer.

$$q_r = -kA\frac{dT}{dr} = -k(4\pi r^2)\frac{dT}{dr} \tag{1.30}$$

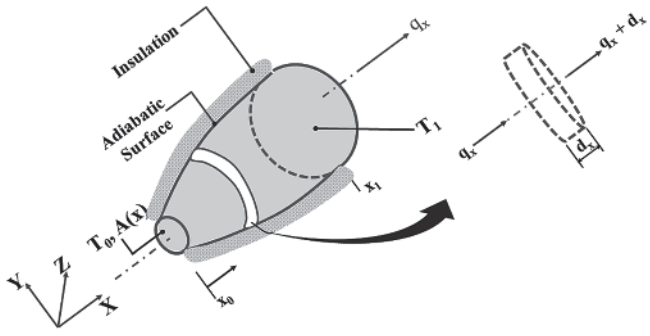

Figure 1.8 Schematic representation of conical nose-tip to determine constant conductive heat transfer rate through the tip.

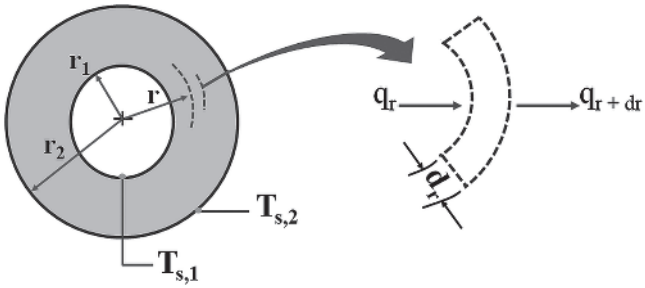

Figure 1.9 Schematic representation of the conduction in a spherical shell.

If q_r is constant and independent of r:

$$\frac{q_r}{4\pi}\int_{r_1}^{r_2}\frac{dr}{r^2} = -\int_{T_{s1}}^{T_{s2}} k(T)dT \tag{1.31}$$

If thermal conductivity, k, is constant:

$$q_r = \frac{4\pi Lk\left(T_{s1} - T_{s2}\right)}{\dfrac{1}{r_1} - \dfrac{1}{r_2}} \tag{1.32}$$

And the thermal resistance $R_{t,\,cond}$ for sphere:

$$R_{t,cond} = \frac{1}{4\pi k}\left(\frac{1}{r_1} - \frac{1}{r_2}\right) \tag{1.33}$$

Other parameters for the spherical composite wall may also be determined as a plane wall and cylinders.

A cumulative list of one-dimensional steady-state heat transfer parameters for three geometries is given in Table 1.2. Herein, the ΔT refers to the difference in temperature $T_{s1} - T_{s2}$ between inner and outer identified surfaces.

1.3.3 Two-Dimensional Steady-state Conduction

One-dimensional steady-state concept allows heat transfer through one coordinate system, but the two-dimensional heat transfer provides better insight and a more accurate heat transfer analysis in advance. Consider a uniform prismatic solid as shown in Figure 1.10, in which the top and bottom are insulated and two sides open with a temperature difference of $T_1 > T_2$, and heat transfers from surface 1 to 2. In consideration of Equations (1.10) and (1.11), the local heat flux in the solid is a resultant vector (q'') of the heat flux of x (q_x'') and y (q_y'') direction, which is anywhere perpendicular to the constant temperature lines.

Table 1.2 One-dimensional steady-state with no heat generation.

	Plane wall	Cylindrical wall	Spherical wall
Heat equation	$\frac{d^2T}{dx^2}=0$	$\frac{1}{r}\frac{d}{dr}\left(r\frac{dT}{dr}\right)=0$	$\frac{1}{r^2}\frac{d}{dr}\left(r^2\frac{dT}{dr}\right)=0$
Temperature distribution	$T_{s,1}-\Delta T\frac{x}{l}$	$T_{s,2}+\Delta T\frac{ln\left(\frac{r}{r_2}\right)}{ln\left(\frac{r_1}{r_2}\right)}$	$T_{s,1}-\Delta T\left[\frac{1-\left(\frac{r_1}{r}\right)}{1-\left(\frac{r_1}{r_2}\right)}\right]$
Heat flux (q'')	$k\frac{\Delta T}{L}$	$\frac{k\Delta T}{rln\left(\frac{r_2}{r_1}\right)}$	$\frac{k\Delta T}{r^2\left(\frac{1}{r_1}\right)-\left(\frac{1}{r_2}\right)}$
Heat rate (q)	$kA\frac{\Delta T}{L}$	$\frac{2\pi Lk\Delta T}{ln\left(\frac{r_2}{r_1}\right)}$	$\frac{4\pi k\Delta T}{\left(\frac{1}{r_1}\right)-\left(\frac{1}{r_2}\right)}$
Thermal resistance ($R_{t,\,cond}$)	$\frac{L}{kA}$	$\frac{ln\left(\frac{r_2}{r_1}\right)}{2\pi Lk}$	$\frac{\left(\frac{1}{r_1}\right)-\left(\frac{1}{r_2}\right)}{4\pi k}$

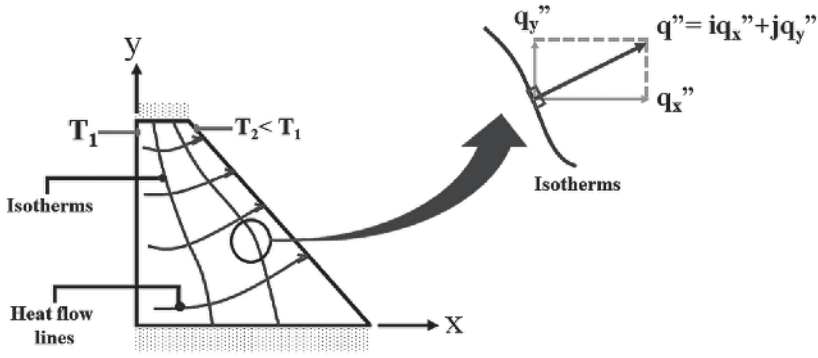

Figure 1.10 Schematic representation for two-dimensional conduction.

The adiabatic surface is usually defined as a boundary where no conduction is across a heat flow line. Thus, the heat equation for an *x-y* plane is:

$$\frac{\partial^2T}{\partial x^2}+\frac{\partial^2T}{\partial y^2}=0 \tag{1.34}$$

Under steady-state conditions, no heat generation and constant thermal conductivity are essential aspects that eventually assist in estimating the "temperature distribution" from the heat equation and "heat flux components" in a two-dimensional system.

The exact mathematical solution of two-dimensional steady-state heat transfer can be determined by analytical, graphical, or numerical methods. In the case of simple geometry, two-dimensional and three-dimensional conduction problems may be easily overcome by using well-documented heat diffusion equations, expressed in terms of shape factor, *S*. However, numerical methods like finite-difference, finite-element with relevant boundary conditions may be used for complex-shaped two-dimensional and three-dimensional geometries to estimate the heat transfer problems. A dimensionless shape factor method may be the rapid solution for the two-dimensional steady-state heat transfer rate calculation by Equation (1.35); where ΔT_{1-2} is the difference in temperature between two boundaries:

$$q = Sk\Delta T_{1-2} \tag{1.35}$$

And the two-dimensional conduction resistance may be expressed as:

$$R_{t,cond(2D)} = 1/kS \tag{1.36}$$

The shape can be obtained analytically and geometrically for several two-dimensional and three-dimensional systems, and a few classic information related to refractory analysis are summarized in Table 1.3.

It isn't easy to estimate the shape factor in some critical conditions. Solving the finite-difference equations by using a numerical method for a nodal network's discrete points is necessary. Further, it is also mandated to consider that various heat transfer processes are time-dependent. Such transient or unsteady incidences arise when the system boundary conditions are changed. For example, a continuous temperature of surface alteration is a common intermittent hot metal billet phenomenon when it comes out from the caster and is exposed to a cool airstream in which the energy is transmitted from its surface to its surroundings through convection and radiation. The conduction process persists from the hot billet interior to the surface until a steady-state condition is reached. The time-temperature history is key to fabricating new materials with tailor-made properties to control the resultant 'performance' of such a process. Considering different heat transfer solutions and numerical approaches, one can estimate and control the properties [1–3].

1.4 Convection

In the previous section, a limited convection heat transfer was considered to emphasize the boundary condition for conductive problems. Usually, convection heat transfer occurs between surface and moving fluid (e.g., air, water, molten metal, etc.) when both have different temperatures. Thus, convection includes energy transfer due to the random motion of adjacent fluid molecules (conduction or diffusion) and

Table 1.3 Conduction shape factors for practical geometries.

System	Schematic	Restrictions	Shape factor S = $q/k(T_1 - T_2)$
Vertical cylinder in a semi-infinite medium	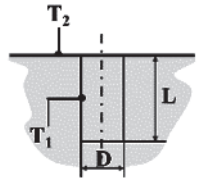	L > D	$\frac{2\pi L}{\ln(4L/\mathrm{D})}$
Circular cylinder of length L centered in a square solid of equal length	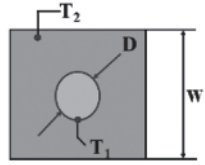	w > D L > w	$\frac{2\pi L}{\ln(1.08w/\mathrm{D})}$
Conduction through the edge of adjoining walls	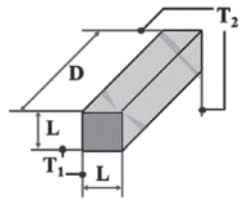	D > 5L	0.54D
Conduction through the corner of three walls with a temperature difference ΔT_{1-2} across the walls	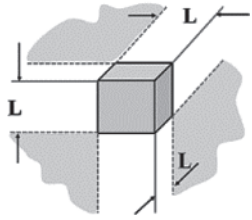	L—length and width of the wall	0.15L
Square channel of length L	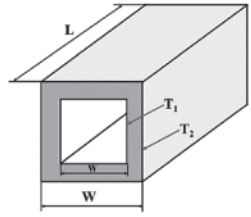	$\frac{W}{W} < 1.4$ $\frac{W}{W} > 1.4$ L > W	$\frac{2\pi L}{0.785\ln(\mathrm{W}/w)}$ $\frac{2\pi L}{0.930\ln(\mathrm{W}/w) - 0.050}$

bulk fluid (advection) due to force and consequent slippage that eventually forms a gradient. Adjacent to the surface, the molecular velocity and temperature remain nearly constant, but both vary and form as a free stream with boundary layers beyond a certain distance. Consequently, fundamentals including a brief of boundary

layers, heat transfer coefficients, laminar and turbulent velocities, internal and external flow, and convection without forced velocity are pointed out.

1.4.1 Boundary Layers

Understanding the boundary layer provides insight into the mass- and heat-transfer between the surface and fluid flowing on it. Convection experiences boundary layers of thermal, concentration, and velocity, and their relationships with heat, mass-transfer, and friction are encountered.

Fluid molecule assumes zero velocity contact to the surface that retards the motion adjoining fluid layer due to shear stress τ parallel to the fluid velocity (u). Such an effect exists up to a certain distance, $y = \delta$, as shown in Figure 1.11. The velocity gradually increases and becomes free stream (∞) with increasing y and follows $u = 0.99u_\infty$ beyond the distance δ. It develops a velocity boundary layer variation with distance from the surface.

This narrow region thickness $\delta = Re_L^{-0.5}$ has sharp velocity gradient. This region is known as hydrodynamic boundary layer region, where Re_L is known as Reynolds number, defined as:

$$\mathrm{Re}_L = \frac{inertia}{viscous\ force} = \frac{u_\infty \mathrm{L}}{\vartheta} = \frac{\rho u_\infty \mathrm{L}}{\mu} \tag{1.37}$$

where, L = length scale, ρ = fluid density, μ = dynamic viscosity of fluid, ϑ = momentum diffusivity or kinematic viscosity. Minute disruptions occur in any flow, which can be intensified to create a turbulent flow. A small Reynolds number (Re_L) experiences high viscous force compared to inertia forces that restrict the laminar to turbulent flow amplification. As Re_L rises at a fixed surface spot, viscous forces have low prominence compared to inertia forces. Therefore, the viscosity of possessions doesn't enter the free stream as far as possible, diminishing the δ value. Fluid flow transport adjacent to surface experiences shear stress, and thus friction, and this friction coefficient (C_f) for external flow depends on:

$$C_f \equiv \frac{\tau_s}{\rho u_\infty^2 / 2} \tag{1.38}$$

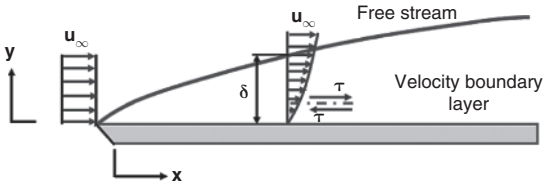

Figure 1.11 Velocity boundary layer on a flat surface.

Assume a Newtonian fluid, the surface shear stress at the surface edge is:

$$\tau_s = \mu \left(\frac{\partial u}{\partial y} \right)_{\gamma=0} \tag{1.39}$$

Usually, the velocity gradient at the surface depends on the distance x from the plate's leading edge in a velocity boundary layer. Eventually, the gradient of velocity and shear stress becomes negligible compared to the adjacent surface in the free stream zone, where fluid viscosity is predominant to encounter the flow analysis.

Similar to the velocity gradient, a sharp thermal gradient experience in the convection process differs from the fluid stream and surface temperature. The temperature profile along the y-axis, $T_y = T_\infty$. However, fluid contact with the plate achieves thermal equilibrium, as shown in Figure 1.12. These fluid molecules exchange heat energy to the adjoining fluid layer, form a thermal boundary with a thickness of δ_t along the y-axis, and follow temperature variation $(T_s - T) = (T_s - T_\infty)\, 0.99$ as similar as velocity difference.

The thermal boundary layer δ_t thickness is equal to $(Re_L.\, Pr)^{-0.5}$, where Pr is the Prandtl number, $c_{p,f}$ = specific heat, and k_f = thermal conductivity of the fluid and can be represented by:

$$\mathrm{Pr} = \frac{momentum\ diffusivity}{thermal\ diffusivity} = \frac{\vartheta}{\alpha} = \frac{\mu/\rho}{k_f/\rho c_{p,f}} = \frac{\mu c_{p,f}}{k_f} \tag{1.40}$$

Momentum diffusivity becomes dominant when $Pr \gg 1$, but the heat diffuses fast compared to fluid velocity in a small value. It implies $\delta_t < \delta$ for oil, $\delta_t \approx \delta$ for gas, and $\delta_t > \delta$ for liquid metal flow adjacent to a flat surface. As the Reynolds number increases, it can also be seen that the boundary layers become narrow, the temperature gradient becomes high, and increases the rate of heat transfer. The local heat flux at any distance x from the leading surface edge strongly influenced by the wall temperature gradient $\partial T / \partial y$ and can be written as:

$$q_s'' = -k_f \left(\frac{\partial T}{\partial y} \right)_{y=0} \tag{1.41}$$

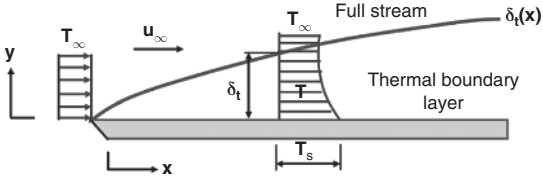

Figure 1.12 Thermal boundary layer on a flat surface.

Employing Newton's law of cooling, the heat flux can be rewritten as similar to Equation (1.15), where $(T_s - T_\infty)$ is constant and independent of x:

$$q''_s = h(T_s - T_\infty) \tag{1.42}$$

From Equations (1.41) and (1.42), we obtain:

$$h = \frac{-k_f \left(\partial T / \partial y\right)_{y=o}}{\left(T_s - T_\infty\right)} \tag{1.43}$$

From Equation (1.43), the magnitude of thermal gradient decreases with increasing *x*, as well as the reduction of q''_s, and *h* with increasing of *x*.

The boundary layer of concentration and mass-transfer of convection exist if the surface species concentration differs from its free stream concentration. In tunnel kiln firing, continuous firing and releasing several volatile and gaseous species results in different near-to-kiln walls and interiors that eventually produce a concentration gradient. Consider a binary mixture of chemical species A (e.g., O_2) and B (e.g., CO_2) that flows over a surface, as shown in Figure 1.13.

The molar concentration (kmol/m^3) of species A at the surface is $C_{A,s,}$ and in the free stream, it is $C_{A,\infty}$. Convection develops a concentration boundary layer from the surface to free stream with a concentration gradient of $(C_{A,s} - C_A) = 0.99\,(C_{A,s} - C_{A,\infty})$, with having a thickness of δ_c, equal to $(Re_L.\ Sc)^{-0.5}$, where Sc is Schmidt number, D_{AB} = mass-diffusivity, where *Sc* is:

$$Sc = \frac{viscous\ diffusion\ rate}{molecular\ (mass)\ diffusion\ rate} = \frac{\vartheta}{D_{AB}} = \frac{\mu}{\rho D_{AB}} \tag{1.44}$$

The Schmidt number measures mass-transport's momentum and relative effectiveness by diffusion in the concentration and velocity boundary layers. Therefore, mass-transfer through convection in laminar flow determines the thickness of boundary layer concentration and relative velocity, $\delta_t/\delta \approx Sc$. The ratio of *Pr* and *Sc* (δ_t/δ_c) known as Lewis number (*Le*) is relevant to any condition requiring simultaneous transfer of mass and heat through convection. Thus, it is the measure of the relative concentration and thermal boundary layer thickness. Analogous to heat flux $N''_{A,s}$, molar flux (kmol/s.m^2) at the surface can be

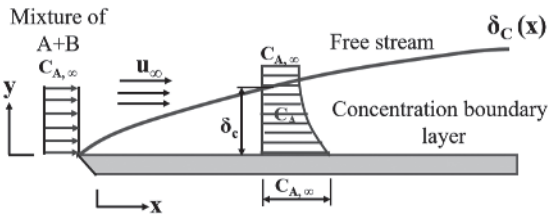

Figure 1.13 Species concentration boundary layer on a flat surface.

represented through Fick's law (Equation 1.45) and Newton's law (Equation 1.46) of cooling, where D_{AB} is the binary diffusion coefficient (mass-diffusivity), and h_m is the convection mass-transfer coefficient:

$$N''_{A,s} = -D_{AB}\left(\frac{\partial C_A}{\partial y}\right)_{y=0} \tag{1.45}$$

$$N''_{A,s} = h_m\left(C_{A,s} - C_{A,\infty}\right) \tag{1.46}$$

From Equations (1.45) and (1.46), the h_m becomes:

$$h_m = \frac{-D_{AB}\dfrac{\partial C_A}{\partial y}}{\left(C_{A,s} - C_{A,\infty}\right)} \tag{1.47}$$

Therefore, the concentration boundary layer conditions strongly affect the surface gradient of concentration and mass-transfer coefficient, hence the species transfer rate in the boundary layer.

Three boundary layers may exist together if temperature and species concentrations are different from the surface to free stream during fluid flow over the surface. The boundary layer velocity is the extent of $\delta(x)$ and is characterized by a velocity gradient. Shear stresses, thermal boundary layer $\delta_t(x)$ is characterized by temperature gradient and heat transfer, and the concentration gradient and species transfer describe concentration boundary layer $\delta_c(x)$. However, the boundary layers hardly develop at the equivalent rate, and the values of δ, δ_t, δ_c at a given location are not the same. The critical boundary layer parameters are coefficient of friction (C_f), coefficients of heat, and mass-transfer convection h and h_m, respectively.

1.4.2 Laminar and Turbulent Flow

It is essential to determine whether the boundary layer is laminar or turbulent flow before deciding the convection problem. Surface friction and the transfer rates of convection strongly depend on which of these conditions occurred.

Figure 1.14a represents a boundary layer formation for both laminar and turbulent flow on a flat plane. The velocity components in the direction of x and y, characterize the motion of the fluid. While the fluid moves away from the surface through x-direction, three distinct zone forms, laminar (1^{st}), laminar to the turbulent transition zone (2^{nd}), and turbulent zone (3^{rd}). Fluid flow is highly ordered within the laminar boundary layer and maintained uniform streamlines along with fluid particles (molecules) move. The local shear stress of the surface reduces with increasing x (Equation 1.39). This behavior continues up to the transition zone where laminar flow converts to turbulent flow, where fluid coexists the dual character of both laminar and turbulent flow.

Beyond the transition zone, the turbulent boundary is highly irregular, and random results bulk three-dimensional flow without maintaining a two-dimensional streamline like laminar flow. In the chaotic flow condition in the turbulent zone, pressure and velocity variations arise at any point within the turbulent boundary layer. Three distinct regions appear as a function of distance from the surface. The "viscous sublayer" is dominated by diffusion where velocity profile is nearly linear, adjoining "buffer sublayer" in which diffusion and turbulence coexist, followed by dominated transport due to the turbulent mixing within the turbulent zone.

A competitive boundary layer of laminar and turbulent profiles for the x-component of the velocity are represented in Figure 1.14b, representing cumulative flow behavior in Figure 1.14a. Laminar to turbulent flow transition is finally due to triggering mechanisms, including unsteady flow that develops naturally within the fluid or minor disturbances within many typical boundary layers.

The onset of turbulence depends on the amplification of triggering mechanisms that eventually depend on the Reynolds number (Equation 1.37). The Reynolds number is small when the inertia forces are negligible compared to viscous forces. The flow remains laminar when the disturbances are dissipated. The inertia forces are high enough for a large Reynolds number to amplify the triggering mechanisms, and a transition to turbulence occurs. Beyond a critical distance x_c, along x-axis persist laminar flow, and the transition begins beyond it.

The fluid flow nature has a significant outcome on mass- and heat-transfer rates. Analogous to the velocity of the laminar layer, the species, and thermal boundary layers propagate in the streamwise (increasing x) direction, gradients of temperature, and species concentration in the fluid at $y = 0$ decrease in the streamwise direction. From Equations (1.43) and (1.47), the mass and heat transfer coefficients also decrease with increasing x. Mixing of turbulence promotes a large concentration gradients of species and temperature adjacent to the solid surface and an equivalent increase in the mass- and heat-transfer coefficients across the region of transition. The cumulative thickness of velocity boundary layer δ and the heat transfer coefficient of local convection h represents a characteristic behavior, as shown in Figure 1.15.

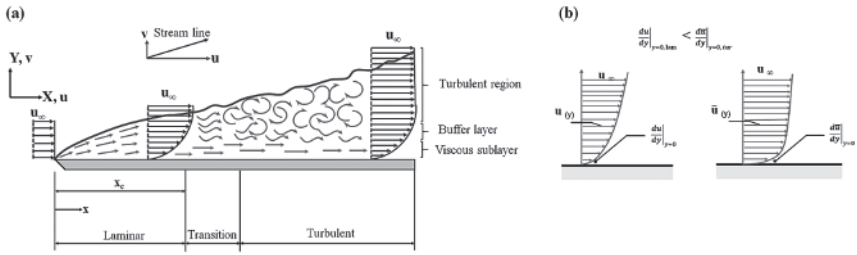

Figure 1.14 (a) Development of velocity boundary layer on a flat plate, (b) comparison of laminar and turbulent velocity boundary layer profiles for the same free stream velocity.

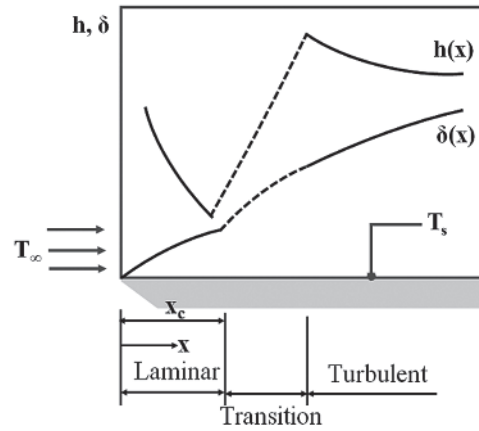

Figure 1.15 Variation of velocity boundary layer thickness δ and the total heat transfer coefficient h for flow over an isothermal flat plate.

The resulting variations in the thickness of the velocity, the species, and the temperature boundary layer appear to be much smaller in the turbulent flow because turbulence causes mixing, which decreases the role of conduction and diffusion in deciding the species and thermal boundary thickness.

1.4.3 Free and Forced Convection

The basic concepts of velocity, thermal, and concentration boundary layer thickness; surface friction coefficient; heat and mass-transfer coefficient; laminar and turbulent flow behavior, and their transition zone in two-dimensional and three-dimensional convection processes; and how these are related to physical parameters such as density, viscosity, thermal conductivity, specific heat, diffusivity, and dimensionless number *Re*, *Pr*, and *Sc* are discussed in the previous section. Bulk fluid motion facilitates the heat transfer and convection mechanism. Convection is further subdivided into two categories: free (or natural), and another is forced convection, based on how the action of fluid originated. In free convection, any fluid motion is initiated by natural means, such as the differences in density and effect of buoyancy, and the rise and fall of warmer and cooler fluid, respectively. Whereas in forced convection, the motion of the fluid is forced to flow over a surface or in a circular section by external agency means a fan or pump. Such a convection process can be observed when air is supplied or extracted by a blower or suction pump into a tunnel kiln to maintain heat and mass-transfer, turbulence in tundish, and subsequent consistent flow control during casting, etc. Forced convection creates a more uniform temperature throughout the entire region. Essential information for the convection in the confined region may provide insight into this understanding and is discussed in the next section.

The convection heat transfer from or to the surface of a material may be calculated using Equation (1.15), and empirical correlation:

$$Nu = cRe^{n}Pr^{m} \tag{1.48}$$

Where Nusselt number (*Nu*) is equal to hL/k, the Reynolds number (*Re*) is $\rho uL/\mu$, and the Prandtl (*Pr*) is $c_p\mu/k$. From Equation (1.49), the free convection coefficient can be estimated:

$$Nu = cRa^n Pr^m \tag{1.49}$$

The Rayleigh number (*Ra*) is $(Ts - T\infty)\beta g\rho L^3/(\alpha\mu)$, where β is the volumetric thermal expansion coefficient, *g* is the gravitational acceleration, ρ is density, *l* is length, and α is thermal diffusivity. The constants *c*, *n*, and *m* for different geometry and flow conditions are available in the literature [4, 5].

1.4.4 Flow in Confined Region

Few real-life incidences represent an example of forced convection during the external flow of fluid. However, several incidences, including molten steel casting, experience confined region flow in a tube such as a slide gate, shroud, subentry nozzle, etc. The boundary layer develops on a surface in external flow and continues without external constraints. In contrast, the pipe's fluid flow cannot form the boundary layer; rather, the hydrodynamic layer's velocity affects the confined flow region. The convection heat transfer coefficients and energy balance are presented for internal flow in the circular channel, considering velocity and thermal boundary layer effects.

Figure 1.16a represents the internal fluid flow entrance and fully developed laminar flow regions with a uniform velocity in a circular tube of radius r_o. Viscous force facilitates the formation of a boundary layer with increasing *x*, which provokes shrinkage of inviscid flow region and subsequent boundary layer merger [6].

Beyond this merger, viscous effects extend over the entire cross-section. In such conditions, the velocity profile becomes unaltered with increasing *x*, and the flow is fully developed, known as hydrodynamic entry length, x_h. The fully developed velocity profile is parabolic for laminar flow in a circular tube, whereas the profile is flatter in the radial direction during turbulent flow. The Reynolds number determines the fully developed internal flow exists as laminar or turbulent flow. The critical Reynolds number ($Re_{D,c}$) for the internal flow near to 2300, where, $Re_{D,c} \equiv \rho u_m D/\mu \approx 2300$, u_m = *mean fluid velocity*, *D* = *tube diameter*. For laminar flow ($Re_D < 2300$), the hydrodynamic length can be calculated from $(x_{e,h}/D)_{lam} \approx 0.05Re_D$, whereas $(x/D) > 10$ indicates the fully developed turbulent flow.

The velocity varies with cross-section and a mean velocity u_m dealing the mass-flow rate during internal flow in the tube. The mass-flow rate is the product of fluid density ρ, mean velocity u_m, and cross-sectional area A_c $(= \pi D^2/4)$, and the Reynolds number can be expressed as Equations (1.50) and (1.51), respectively:

$$\dot{m} = \rho u_m A_c \tag{1.50}$$

$$Re_D = \frac{4\dot{m}}{\pi D\mu} \tag{1.51}$$

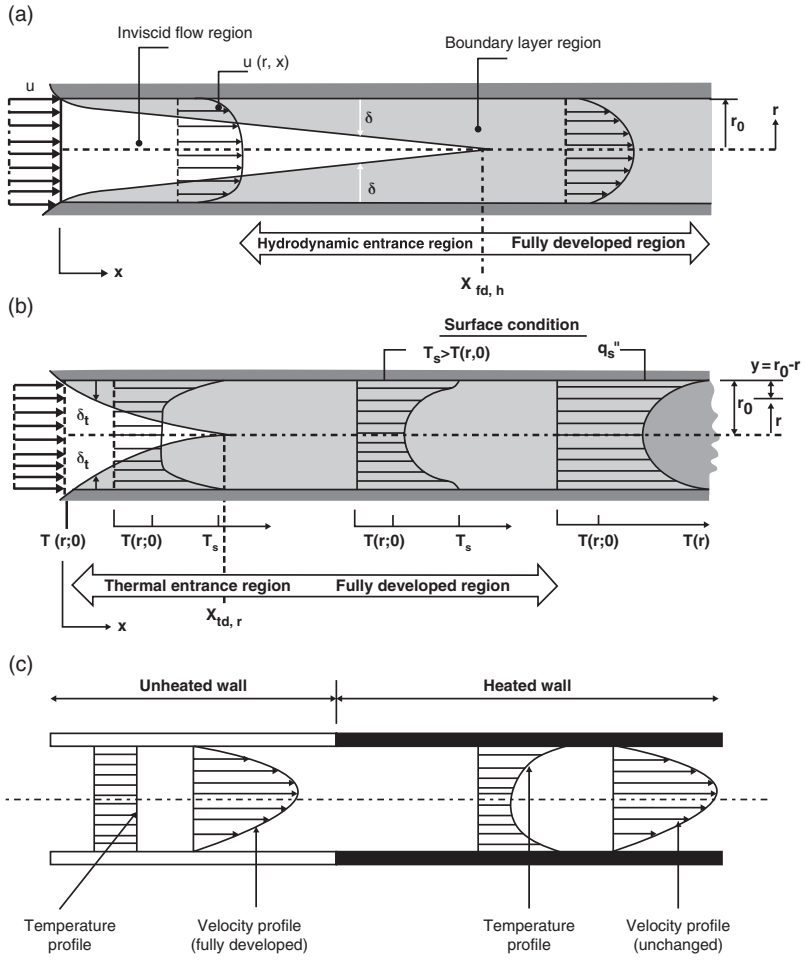

Figure 1.16 (a) Laminar, hydrodynamic boundary layer development in a circular tube, (b) thermal boundary layer development in a heated circular tube, (c) variation of temperature and velocity profile for an unheated and heated wall.

The velocity profile may readily be determined for the laminar flow of an incompressible, constant property fluid fully developed region. The resultant velocity concerning r may also be determined from Equation (1.52):

$$u(r) = 2u_m \left[1 - \left(\frac{r}{r_o}\right)^2\right] \tag{1.52}$$

Pressure drop is a common incidence due to friction, and Moody (or Darcy) friction factor f for fully developed laminar flow becomes:

$$f = 64/\mathrm{Re}_D \tag{1.53}$$

however, the analysis of friction factors for turbulent flow relies on experimental data. In approximate, the *f* for turbulent flow follows the relation:

$$f = (0.790 \ln Re_D - 1.64)^{-2}, \textit{where } 3000 \le Re_D \le 5\times10^6 \tag{1.54}$$

Despite fluid velocity gradient, a thermal boundary layer is shown in Figure 1.16b when fluid enters at a uniform temperature $T(r,0)$ less than surface temperature and gradually increases with x. The shape of the hydrodynamically fully developed temperature profile $T(r,x)$ differs according to whether a uniform surface temperature (UST) or uniform heat flux (UHF) is maintained. The characteristic velocity and temperature profile concerning the heating condition is shown in Figure 1.16c. For laminar flow, the thermal entrance length may be expressed as:

$$\left(\frac{x_{e,t}}{D}\right)_{lam} \approx \begin{cases} 0.033 Re_D \mathrm{Pr} \ \textit{for UST} \\ 0.043 Re_D \mathrm{Pr} \ \textit{for UHF} \end{cases} \tag{1.55}$$

We can generalize, $(x_{e,t}/D) = 0.05\ Re_D\ Pr$. Under the circumstance of $Pr > 1$, the hydrodynamic boundary layer develops more rapidly than the thermal boundary layer x_h (velocity profile) $< x_{e,t}$ (thermal profile), then $\delta > \delta_T$ at any section; while the inverse is true for $Pr < 1$. For extensive Prandtl number fluids, such as oils ($Pr \ge 100$), $x_{e,h}$ is much smaller than $x_{e,t}$, and it is reasonable to assume a fully developed velocity profile throughout the thermal entry region. In contrast, conditions are nearly independent of the Prandtl number for turbulent flow, and to a first approximation, $(x_{e,t}/D) = 10$. The bulk mean temperature (T_m) at any section (x) is given by:

$$T_m = \frac{2}{u_m r_o^2} \int_0^{r_o} u(r) T(r) r dr \tag{1.56}$$

By employing Newton's law of cooling, the heat flux is $q''_s = h(T_s - T_m)$, where h is the local convection heat transfer coefficient. The value of T_m increases with x if heat transfer is from the surface to the fluid ($T_s > T_m$); it decreases with x if the opposite is true ($Ts < Tm$).

In a confined region, as shown in Figure 1.17, the $T_m(x)$ varies with position along the x, and the total q_{conv} is related to the difference in temperatures at the tube inlet ($T_{m,i}$) and outlet ($T_{m,o}$), constant flow rate $\dot{m}$ and specific heat capacity of the fluid. In steady-state flow conditions, the convection heat transfer can be written as Equation (1.57):

$$q_{conv} = \dot{m} c_\rho \left(T_{m,o} - T_{m,i}\right) \tag{1.57}$$

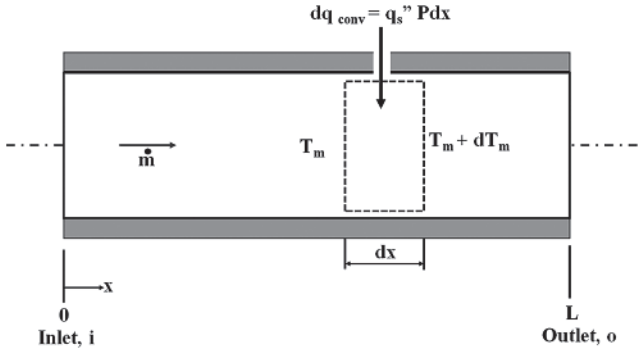

Figure 1.17 Control volume for flow in a confined region.

The rate of thermal energy advection integrated over the cross-section:

$$dq_{conv} = q_s'' P dx = \dot{m} c_\rho \left[\left(T_m + dT_m \right) - T_m \right] \tag{1.58}$$

The heat flux $q_s^{"} = dq_{conv} / Pdx$, where $P = surface\ perimeter = \pi D$ for a circular tube. From the combination of Equations (1.42) and (1.58), we may obtain:

$$\frac{dT_m}{dx} = \frac{q_s'' P}{\dot{m} c_\rho} = \frac{P}{\dot{m} c_\rho} h \left(T_s - T_m \right) \tag{1.59}$$

This expression is a beneficial result, from which the axial variation of Ts may be determined. If $T_s > T_m$, heat is transferred to the fluid, and T_m increases with x; *if* $T_s < T_m$, the opposite is true. The convection coefficient is constant in the fully developed region, and it varies with x in the entrance region. The $T_m\ (x)$ depends on two special cases, constant surface heat flux and constant surface temperature.

For constant surface heat flux, the $q_s^{"}$ is independent of x, and follows $q_{conv} = q''_s (P.L)$ and equating with Equation (1.57), followed by integrating results

$$T_m \left(x \right) = T_{m,i} + \frac{q''_s P}{\dot{m} c_\rho} x \tag{1.60}$$

$$q''_s = constant$$

Equation (1.60) reveals that the mean temperature varies linearly with x along the tube and same time variation of $(T_s - T_m)$ with x as shown in Figure 1.18a. Due to the significant value of h near the entrance, the difference is negligible at starting

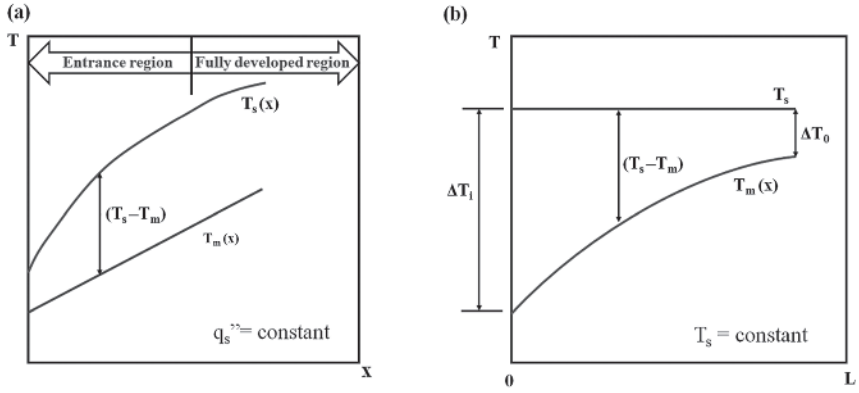

Figure 1.18 Axial temperature variation for heat transfer in a tube (a) constant surface heat flux, (b) constant surface temperature.

but increases with x, the increase owing to the reduction in h that occurs as the boundary layer grows. In reality, the h is independent of x in the fully developed region; thus the $(T_s - T_m)$ is independent of x in this region.

While considering the uniform temperature of the surface, the total rate of heat transfer and axial distribution follows exponential decay and depends on the average coefficient of heat transfer $(\bar{h})$, the resultant relation can be expressed as:

$$\frac{\Delta T_o}{\Delta T_i} = \frac{T_s - T_m(x)}{T_s - T_{m,i}} = \exp\left(-\frac{Px}{\dot{m}c_\rho}\bar{h}\right) \tag{1.61}$$

$$T_s = constant$$

Thus, the difference in temperature $(T_s - T_m)$ decays exponentially with distance along the tube axis, and thus the axial surface and distributions of average temperature are as shown in Figure 1.18b.

Despite the circular cross-section, several engineering applications demand convection transport in noncircular tubes. Many of the circular tube results may be applied by using an effective diameter as the characteristic length to determine the Re_D and Nu_D. In a simple way, this effective diameter of hydraulic is defined as:

$$D_h \equiv \frac{4A_c}{P} \tag{1.62}$$

Where A_c and P are the cross-sectional flow area and the wetted perimeter, respectively. For laminar flow, circular tube correlations are less accurate when the system has sharp corners. For such cases, the details of the Nusselt number

corresponding to fully developed conditions may be obtained from detailed analysis in literature [7].

1.5 Radiation

Conduction and convection both process experience temperature gradient; however, the radiation is an important heat transfer mode for much industrial heating, cooling, and drying processes as well as energy conversion involved with fossil fuel combustion and solar radiation.

1.5.1 Basic Concepts

All forms of matter emit radiation. The emission mechanism is related to energy released due to transitions or oscillations of the electrons present in the material. These oscillations are in turn persistent by the emission of internal energy as thermal radiation, and therefore the temperature of the matter. Hence, the emission of thermal radiation with thermally excited conditions within the matter. At elevated temperatures, the emission is a volumetric phenomenon; however, the discussion only focuses on radiation through the surface. Accordingly, radiation emitted from a solid or a liquid originates from molecules within an approximate distance of 1 μm from the exposed surface.

Despite the situation in nanoscale or microscale devices, emission from a solid or a liquid toward adjacent gas or a vacuum can be viewed as a surface phenomenon. Emission does not require the presence of matter, may happen in a vacuum; thus radiation is the result of the propagation of collective particles known as *photons* or quanta or defined as the propagation of electromagnetic waves. For radiation propagating in a particular medium, the wavelength:

$$\lambda = \frac{c}{V} \tag{1.63}$$

Where c is the speed of light in the medium. For propagation in a vacuum $c_o = 2.998 \times 10^8$ m/s. Wavelength (λ) variation for *thermal radiation* in the range of 0.1–100 μm includes a portion of UV and all visible and infrared (IR) pertinent to heat transfer. Thermal radiation emitted by a surface encompasses a range of wavelengths. The magnitude of the radiation varies with wavelength, and the term spectral is used to refer to the nature of this dependence. Emission follows the directional distribution of the emitted radiation with radiation intensity.

1.5.2 Emission from Real Surfaces

A blackbody is an ideal emitter as it can emit maximum radiation compared to any other material at the same temperature. Planck's law describes the spectral density

of electromagnetic radiation emitted by a black body in thermal equilibrium at a given temperature T. The emissivity and temperature can be correlated as Equation (1.64), where $\sigma = 5.67 \times 10^{-8}$ W/m^2.K^4, known as Stefan–Boltzmann constant:

$$E = \sigma T^4 \tag{1.64}$$

Thus, emissivity may be defined as the ratio of the radiation emitted by the surface to the radiation emitted by a black body at the same temperature. Spectral radiation distribution, as well as directional distribution for real surface emission, are different from Planck distribution of a black body, as shown in Figures 1.19a and 1.19b.

Representative spectral distribution of ε_λ (spectral emissivity) varies for a conductor, nonconductor, and nature of the surface coating (like the presence of oxides), as shown in Figure 1.20a. Total normal emissivity concerning temperature for a different material class is shown in Figure 1.20b [6].

The available data demonstrates that the emissivity of metallic surfaces is generally small, as low as 0.02 for polished metal surfaces. A classical analysis and derivation represent emissivity of a material and is inversely proportional with thermal conductivity, and it can be represented by Equation (1.65) where, k = thermal conductivity:

$$\varepsilon_n = 0.865X10^{-4}\ k^{-1/2} \tag{1.65}$$

At the same time, the oxide layer increases the emissivity of metal surfaces; at elevated temperatures, the stainless steel becomes oxidized, and emissivity increases from 0.3 to 0.7.

In this contrast, the emissivity of nonconductors is comparatively large, generally more than 0.6. The emissivity of conductors increases with increasing temperature; however, depending on the specific material, nonconductors' emissivity may either increase or decrease with increasing temperature. Emissivity strongly depends on the nature of the surface, which can be influenced by the method of fabrication, machining and polishing, thermal cycling, and chemical reaction with its environment.

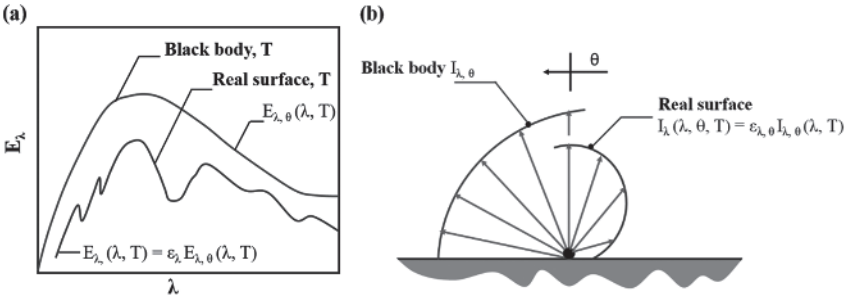

Figure 1.19 Comparison of a black body and real surface emission, (a) spectral distribution, (b) directional distribution.

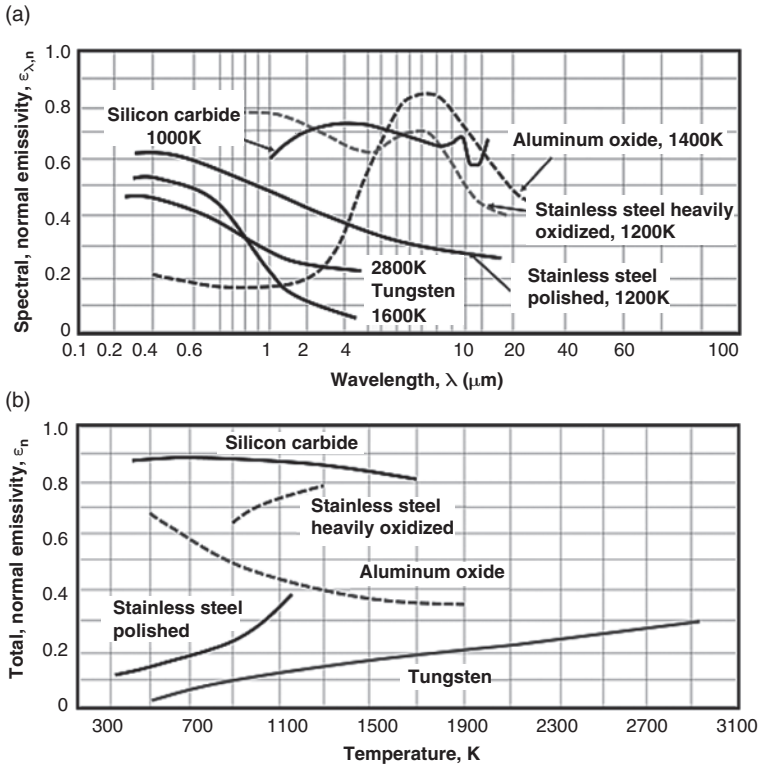

Figure 1.20 (a) Spectral dependence of the spectral, normal emissivity $\varepsilon_{\lambda\text{-}n}$, and (b) temperature dependence of the total, normal emissivity ε_n of selected materials.

1.5.3 Absorption, Reflection, and Transmission by Real Surfaces

Many substances, especially metal oxides, are semitransparent in the visible and infrared spectral ranges.

Let's consider how certain irradiation of wavelength (λ) interacts with a semi-transparent medium like fused quartz; part of the radiation may be absorbed, reflected, and transmitted represented in Figure 1.21, and can be represented as:

$$G_\lambda = G_{\lambda,\text{ref}} + G_{\lambda,\text{abs}} + G_{\lambda,\text{tran}} \tag{1.66}$$

The $G_{\lambda,tran}$ becomes zero for opaque materials, most engineering material. The remaining absorption and reflection processes may be considered as surface phenomena. However, there is no net effect of the reflection process on the medium, while absorption increases the medium's internal energy. Thus, surface absorption and reflection are responsible for the perception of color. Unless the surface is at a high temperature ($T_s \geq 1000$ K), such that it is incandescent, color is in no way due to emission, which is concentrated in the *IR* region and is hence invisible to the eye.

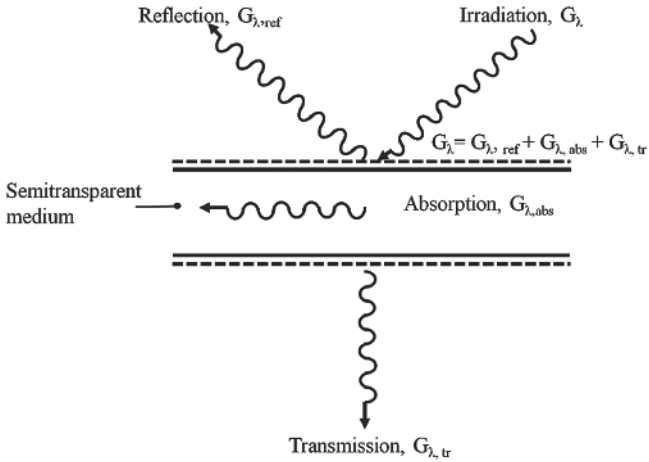

Figure 1.21 Absorption, reflection, and transmission processes associated with a semitransparent medium.

Spectral distributions of the normal reflectivity and absorptivity are plotted in Figure 1.22a for some opaque materials. A material such as glass or water, semitransparent at short wavelengths, becomes opaque at longer wavelengths.

This behavior is shown in Figure 1.22b, representing the spectral transmissivity of several common transparent materials. It is to be noted that inclusion has a significant effect on the resultant transmissions.

1.5.4 Exchange Radiation

Exchange radiation encounters the radiation between two solid surfaces, liquid and polar gases, such as CO_2 and H_2O vapor. The exchange radiation phenomenon depends on the surface geometries and orientations and their radiative properties and temperatures. In an enclosure of two surfaces, the multiple reflection and absorption facilitate radiation exchange between two surfaces.

Consider the enclosure of two surfaces, as shown in Figure 1.23, where radiation is involved within each other. The existence of two such surfaces' net radiant heat must be equal, and in this circumstance, the rate of heat radiation from surface 1 is q_1, equal to the q_2, net rate of radiation transfers to surface 2.

This indicates $q_1 = -q_2 = q_{12}$. The net radiation exchange between surfaces may be expressed as:

$$q_{12} = q_1 = -q_2 = \frac{\sigma\left(T_1^4 - T_2^4\right)}{\frac{1-\varepsilon_1}{\varepsilon_1 A_1} + \frac{1}{A_1 F_{12}} + \frac{1-\varepsilon_2}{\varepsilon_2 A_2}} \tag{1.67}$$

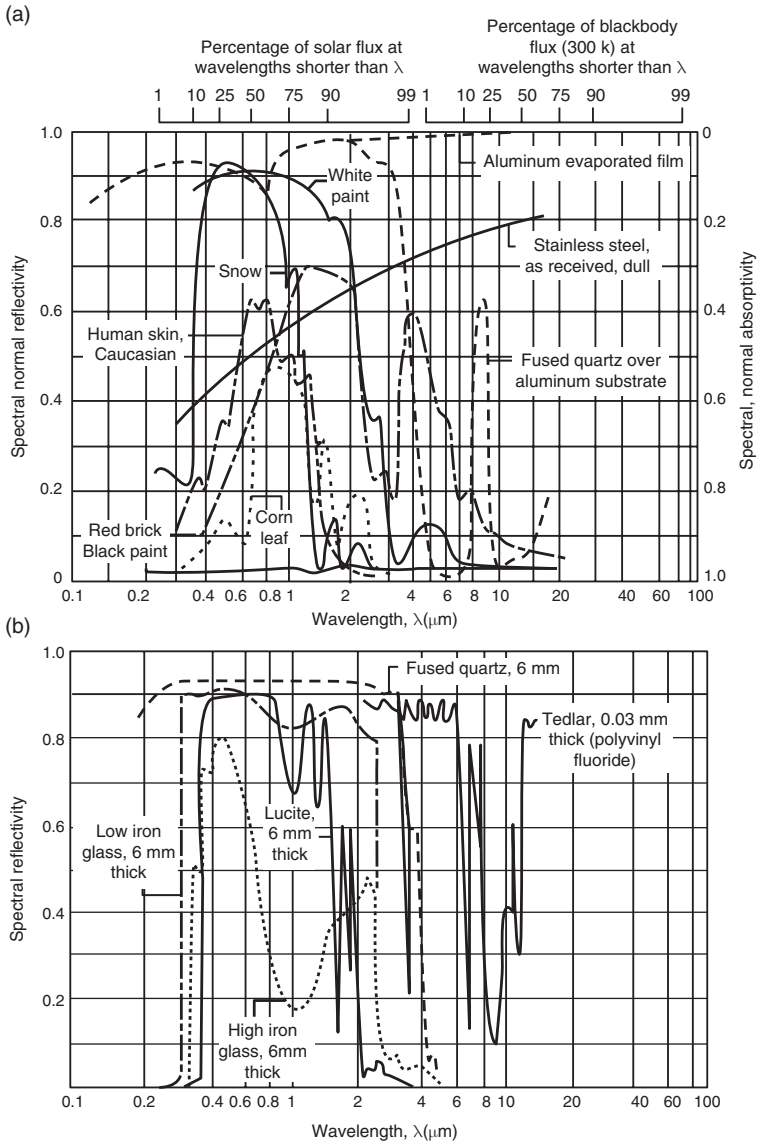

Figure 1.22 Spectral dependence of the spectral, (a) normal absorptivity and reflectivity of opaque materials, (b) transmissivities of semitransparent materials [6] / John wiley & sons.

Where A_1, ε_1, T_1 and A_2, ε_2, T_2 are the surface area, emissivity, and temperature of surfaces, respectively. The view factor F_{12} is the fraction of energy exiting an isothermal, opaque, and diffuse surface 1 (by emission or reflection) that directly impinges on surface 2.

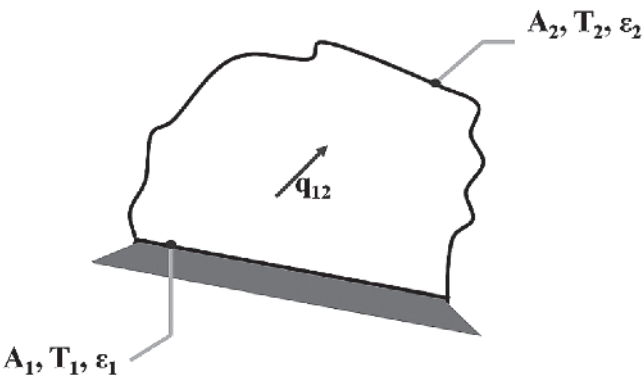

Figure 1.23 Schematic representation of the two surfaces enclosure.

The radiation is not a surface phenomenon for liquid and gaseous, rather more apposite as a volumetric phenomenon. Emission from the gas per unit area of the surface is expressed as Equation (1.68), where E_g is gas emissivity:

$$E_g = \varepsilon_g \sigma T_g^4 \tag{1.68}$$

The rate of radiant heat transfers to a surface due to emission from an adjoining gas is Equation (1.69), where A_s is surface area:

$$q = \varepsilon_g A_s \sigma T_g^4 \tag{1.69}$$

In the same chronology, the net flow rate of thermal radiation energy between a volume of gas and the wall encloses the gas space, where A_v is geometry-dependent absorptance:

$$\dot{Q}_{gw} = A\sigma \frac{\varepsilon_w}{1-\left(1-\varepsilon_w\right)\left(1-A_v\right)} \left(\varepsilon_g T_g^4 - A_v T_w^4\right) \tag{1.70}$$

It is valid only if the temperature, density, and concentration of the gas are constant in space, and its application requires knowledge of the gas emissivity and absorbance.

1.6 Mass Transfer

Modes of mass-transfer are similar to heat transfer. The temperature difference in a medium is the prime driving force for heat transfer; in the same analogous concept, the concentration gradient of chemical species facilitates mass-transfer. Some important aspects related to convection and multiphase mass-transfer are discussed.

1.6.1 Convection Mass Transfer

Some relevant understanding and equations for convection mass-transfer have already been discussed in Section 1.4.1; however, an additional piece of information may provide better insight into the subject. Mobile interface separates two immiscible moving fluids or boundary surface and a moving fluid. In contrast, consider the refractory interaction with molten metal, the convection analysis between the fixed solid surface, and moveable fluid is more important than bulk fluid. Convection mass-transfer is of two types, forced convection, and natural convection. The rate equation for both forced and natural convective mass-transfer is:

$$N_A = k_c \Delta C_A \tag{1.71}$$

Where N_A is the molar-mass flux of species A, ΔC_A is the difference between the boundary surface concentration and the average concentration of the diffusing species in the moving fluid stream, and k_c is the convective mass-transfer coefficient. It defines the mass-transfer rate per unit area per unit driving force and indicates how fast the mass-transfer is by convection. In heat transfer, the ratio of molecular mass-transport resistance to the fluid convective mass-transport resistance is known as the Sherwood number, *Sh*, and analogous to the Nusselt number *Nu*. Sherwood number is:

$$Sh = \frac{molecular\ mass\ transport\ resistance}{convective\ mass\ transport\ resistance} = \frac{k_c L}{D_{AB}} \tag{1.72}$$

$Sh = 1$ provides that the diffusion coefficient (mass-diffusivity, D_{AB}) is equal to the product of characteristic length, L (depends on the geometry), and mass-transfer coefficient (k_c). In another way, the dimensionless Lewis (*Le*) number can be defined as the ratio of thermal diffusivity to mass-diffusivity encountered during the simultaneous convective transfer of mass and energy.

A few significant mass-transfer correlations for different geometries during laminar and turbulent flow are summarized in Table 1.4.

1.6.2 Multiphase Mass Transfer

In multiphase systems, the rate of species mass-transfer is governed not only by the temperature and pressure of the system but also by the mass-transfer conductance, gradients of concentration, kinetics by reaction, activation energy, etc. In a few circumstances, any mass-transfer conductance or kinetics by reaction could control the overall mass-transfer rates; the lowest will be the limiting rate or controlling step. Many theories deal with the mass-transfer among phases, such as the two-film, penetration, and surface renewal approaches. The oldest two-film

Table 1.4 Dimensionless number correlations for mass-transfer in laminar and turbulent flow.

Geometry	Correlations	Conditions
Flat surface	$Sh_L = 0.664\ Re_L^{0.5}\ Sc^{0.33}$ $Sh_L = 0.664\ Re_L^{0.5}\ Sc^{0.33}$	(laminar) $Re_L < 2 \times 10^5$ (turbulent) $Re_L > 2 \times 10^5$
Solid cylinder immersed in water	$kc\ Sc_{0.56}/V_\infty = 0.281\ Re_D^{-0.4}$	(turbulent); $400 < Re_D < 25{,}000$ and $0.6 < Sc < 2.6$
Flow-through pipe	$Sh = 0.032\ Re0.8\ Sc0.33$	$2000 < Re_D < 35000$ and $1000 < Sc < 2260$

theory for gas-liquid mass-transfer assumes the existence thickness of a film *(δ)* in both the liquid and gas phases divided by an interface. According to the following assumptions: (1) the transfer of mass occurs by molecular diffusion through the film, beyond which the concentration (C_{Ab}) is homogeneous; (2) under the steady-state conditions, the transfer of mass occurs through the film; and (3) the transfer of mass occurs at low concentration when the flux is small.

The concentration profile is thus linear for convective mass-transfer as shown in Figure 1.24, and the coefficient of liquid side mass-transfer is expressed by Equation (1.73):

$$kL = \frac{D_{AB}}{\delta_L} \tag{1.73}$$

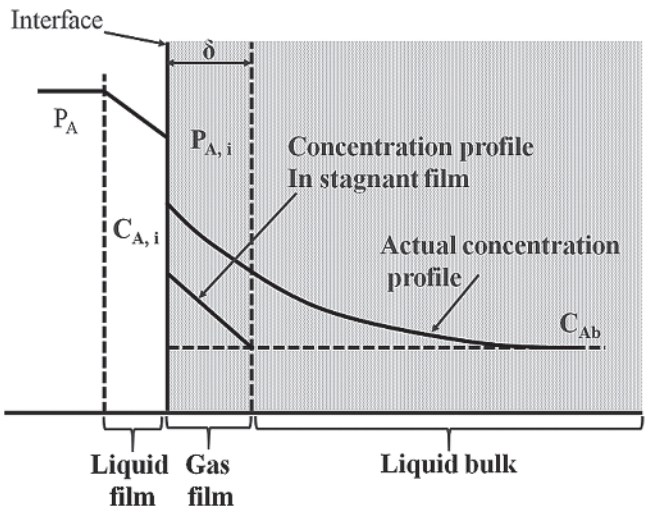

Figure 1.24 Schematic of two-film theory.

Where D_{AB} is the molecular diffusivity of the gas (solute A) into the liquid (solvent B), k_L is proportional to the diffusivity of the power one. The diffusivity primarily depends on the temperature, solvent viscosity, composition, and nature of the solvent. Several investigations established a relation with k_L and D_{AB} from experimental observations in $k_L \propto (D_{AB})^{\mathrm{m}}$, where the $^{\mathrm{m}}$ value varies 0.33–0.66.

1.6.3 Analogy—Heat, Mass, and Momentum Transfer

Dimensionless equations become analogous if both of the same forms govern two or more processes. Analogies between the transfer of mass, heat, and momentum originate in the statistical explanation of the effects or the physical parameters used for the quantitative description. It is known that the mass-diffusion and heat conduction have similar equations to explore these analogies. Specifically, Fick's Law describes the diffusion in one dimension as:

$$J_A = -D_{AB}\frac{dc_A}{dz} \tag{1.74}$$

Similarly, Fourier's law describes heat conduction, where k is the thermal conductivity:

$$q = -k\frac{dT}{dz} \tag{1.75}$$

A similar equation, Newton's law, describes the momentum transfer:

$$\tau = -\mu\frac{du}{dz} \tag{1.76}$$

Where momentum flux (or shear stress) is $\tau_{s,}$ and viscosity of a fluid μ.

It has become conventional at this stage to draw an analogy between the transfer of mass, heat, and momentum. A simple law combined with a balance of mass or energy, or momentum is used by each process. Several analogies are considered among transfer phenomena suggested due to the similarity in their mechanisms in this section. The analogies help to understand the transfer phenomena and as a satisfactory means of assessing the safety of systems for which minimal quantitative data is available. Accordingly, the similarity of the transfer phenomena and the presence of the analogies requires that the five primary following conditions exist within the system.

1) The constant physical properties.
2) There is no reaction chemically within the system due to no mass or energy induced.

3) There is no absorption or emission of radiant energy.
4) There is no dissipation of viscous energy.
5) Velocity profile does not affect the mass-transfer rate; thus mass-transfer rate is low.

Reynolds, known as the Reynolds analogy, established a common analogous mass, heat, and momentum transfer behavior. Although this analogy is limited to gases, a further modification was done by the Chilton–Colburn analogy considering all fluids, gases, and liquids. Reynolds suggested that the mass, momentum, and energy transfer mechanisms are similar and indicate a clear relationship between the various transport phenomena. Correspondingly:

$$\frac{k_c}{u_\infty} = \frac{h}{\rho u_\infty c_\rho} = \frac{f}{2} \tag{1.77}$$

Where h is a heat transfer coefficient, f is the friction factor, u_∞ is the velocity of the free stream. This relation is found to be accurate when Prandtl ($Pr = c_p\mu/k$) and Schmidt ($Sc = \mu/\rho D_{AB}$) are equal to one. The mass-transfer coefficients from the heat transfer coefficient can be calculated during turbulent eddies in gases. In the *Chilton–Colburn analogy*, there are no restrictions on the unit values of Prandtl and Schmidt numbers. These are defined through j factor for mass-transfer as j_D and heat transfer as j_H, and can be written as:

$$j_D = \frac{k_c}{u_\infty} Sc^{2/3} \tag{1.78}$$

$$j_H = StPr^{2/3} \tag{1.79}$$

St. refers to the Stanton number:

$$St = \frac{Nu}{RePr} = \frac{h}{\rho u_\infty c_\rho} \tag{1.80}$$

Exhaustive data for both laminar and turbulent flow regimes established:

$$j_D = j_H = \frac{f}{2} \tag{1.81}$$

This analogy is valid for gases and liquids within the range of $0.6 < Sc < 2500$ and $0.6 < Pr < 100$. The Chilton–Colburn analogy is valid for much different geometry, for example, flow over flat plates (refractory lining), flow in pipes (during casting), and flow around cylinders (submerged monoblock stopper). While

comparing the equations relating to heat and momentum transfer with heat and mass-transfer, it can be shown that:

$$\left[\frac{h_c}{\rho c_p h_m}\right] = \left[\frac{\alpha}{D}\right]^{\frac{2}{3}} \tag{1.82}$$

The above analogies are especially useful when implemented, and if the friction factor is known, it is also helpful to determine the heat transfer coefficient. From the information of heat transfer coefficient, the mass-transfer coefficient can be determined.

1.7 Heat Transfer in Refractory Lining

The heat transfer analysis for multilayer refractory lining in both transient and continuous operation is critical to optimize the working and backup lining with knowledge of their physical, thermal, and mechanical properties. An optimum lining provides consistent performance. Insulating refractories are thermal barriers that keep in the heat and save energy. As the cost of energy has increased, the role of insulating refractories has become more important. Determining temperature profile through different layers either in a kiln, a refractory manufacturing unit, or ladle, the steel manufacturing unit is essential for design and operational troubleshooting. From the perspective of structure and energy efficiency, the design of refractory linings is becoming increasingly important for effective operation practice. Strict "fitness for service" (FFS) guidelines for pressure vessels must be maintained to provide the plant's safety, including assets and public health. Knowing accurate thermal property and convection/radiation boundary conditions makes it possible to predict temperature profiles under various conditions with reasonable accuracy. An optimum thickness is necessary to enhance the refractory life. For example, low insulation thickness may facilitate the buckling of steel ladle and hot spot on the outer shell when the temperature is > 370 ^{o}C, but more insulation thickness can overheat the working lining; thus rapid oxidation and corrosion of MgO-C brick in contact with steel. The thumb rule says that just a 50 ^{o}C increment of working lining temperature may boost the refractory's double corrosion rate.

1.7.1 Tunnel Kiln

A well-established tunnel kiln provides continuous high output. Excellent thermal insulation of the walls enhances the efficiency of the modern kiln. They also use lighter support materials on the car floor, reducing the thermal inertia of assembly. The high efficient kiln can be programmed for faster firing cycles without any

critical restrictions imposed by the particular features of loaded refractory. The sketch in Figure 1.25a is related to the transversal section of the kiln in the firing zone for effective heat transfer in the entire inner space and minimum heat loss through the kiln [8]. The combustion process produces high-temperature gases that pass through the whole chamber. Such a process is responsible for different degrees of energy transfer processes, and these are listed as follows:

- Radiation and conduction between the loaded refractories;
- Radiation and conduction between the refractories of car and load;
- Radiation between the outside loaded refractories and the kiln structure inner surface;
- Convection inner and outer of the loaded refractories with the gases due to combustion;
- Radiation between the surface of car and base of the kiln;
- Convection between car and kiln car base;
- Effective conduction in between kiln walls;
- Convection between the inner surfaces of the wall and flowing gases inside the tunnel; and
- Radiation and convection between the wall outer surfaces and the environment.

The influence of insulation lining is demonstrated in Figure 1.25b. A typical temperature profile for insulated and non-insulated refractory lining exhibits the load temperature difference considering the same amount of fuel consumption and cumulative refractory thickness.

Non-insulated lining governs lower temperature distribution, and thus a bulk amount of energy is lost to the outside ambient. Indeed, bulk energy will be required to stimulate the firing process, and a smaller amount of energy can be recovered at the dryer in the cooling zone. Systematic heat transfer analysis may assist in designing and selecting the refractory for such kiln lining.

1.7.2 Ladle Lining

Steel ladles, composed of refractories and steel construction components, act as transportation vessels and refining units for the steel-melting shop. Refractory linings act as insulating lining and protect the steel shell and consecutive heat loss through the shell despite the working lining. A well-lined steel ladle offers efficient temperature control of the steel melt and adequate steel quality and productivity. A typical steel ladle lining consisting of metal/slag working zone MgO-C, backup LCC-70, and flow control system is shown in Figure 1.26a. It experiences several heat transfer phenomena during different operational conditions. In the steel-melting shop (SMS) the ladle is continuously used for molten metal transport for casting. Uninterrupted operation without delaying ladle engagement is always a challenging task for SMS [9].

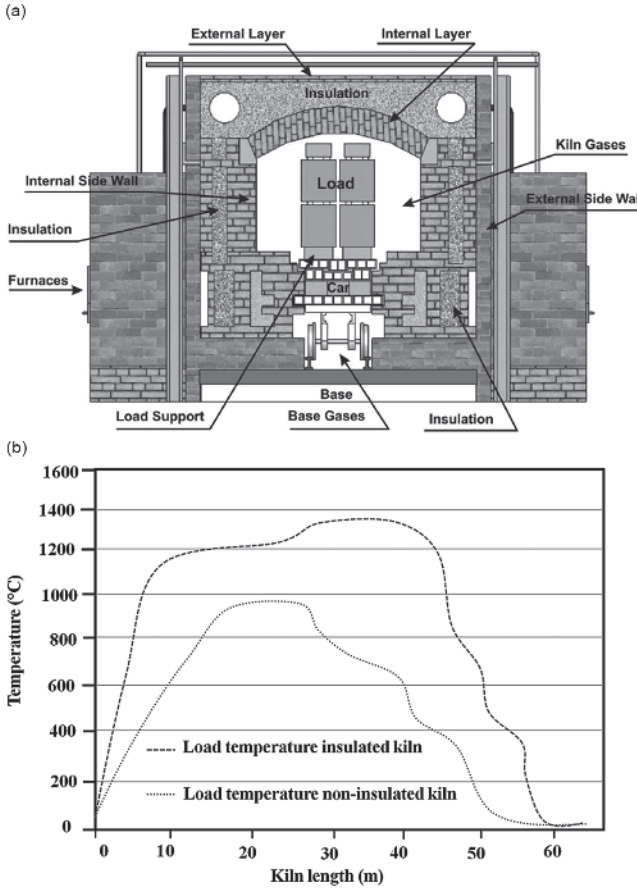

Figure 1.25 A typical representation of (a) tunnel kiln cross-section consists of refractory lining pattern, refractory loading pattern in the car for effective performance, (b) effect of kiln insulation on the central temperature up to maximum 1100 °C [8] / ABCM.

Several unavoidable issues such as delay in ladle lining, different preheating sequence, empty ladle, or idle time may severely affect and delay operation that eventually changes the temperature profile of refractory lining and affects bricks' life. In this context, a typical temperature profile variation for different preheating times and empty ladle times is shown in Figure 1.26b. Consider an empty time of 30 minutes, after which the hot face temperature has fallen significantly, but the temperature profile in the working lining is still high. Thus, immediate preheating is mandatory to increase the hot face temperature by flame temperature. Low heat flux occurs when the temperature gradient becomes small between the lining and flame. As the safety lining and working

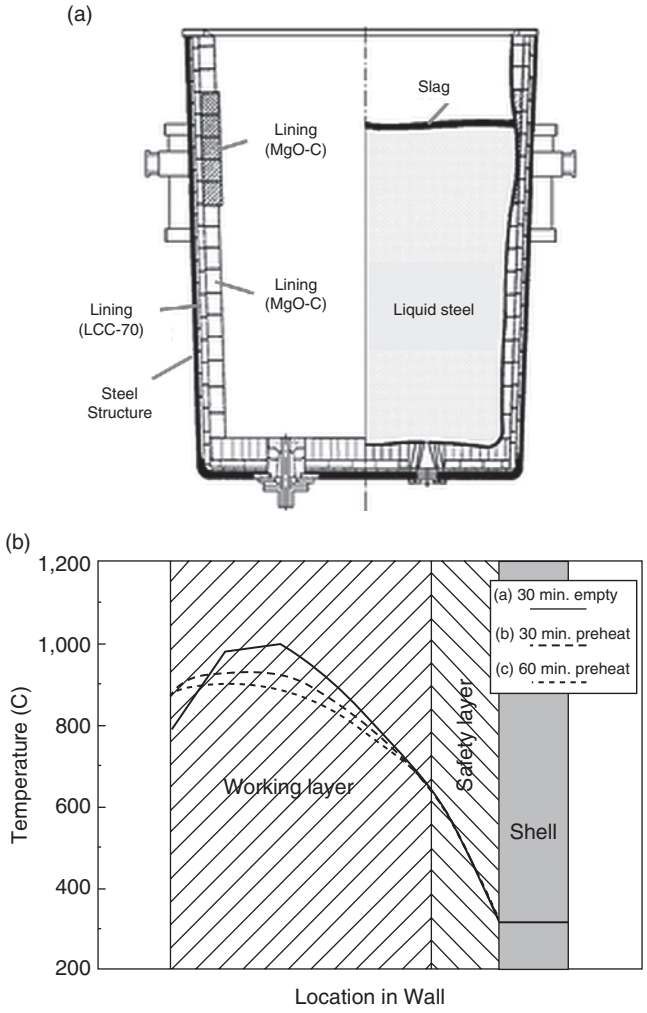

Figure 1.26 A typical schematic representation of (a) steel ladle lining consisting of MgO-C (working), LCC-70 (backup), and different flow control arrangements, (b) temperature profiles in the ladle lining for different preheating and empty times.

heat content remain virtually unaffected, heat loss to the surrounding occurs through the steel shell. Analogous to this incidence and operating conditions, a detailed temperature profile and heat transfer understanding may assist in designing the steelmaking refractories and discussed in Chapter 8.

References

1 Carslaw, H.S. and Jaeger, J.C. (1986). *Conduction of Heat in Solids*, 2e. London: Oxford University Press.

2 Yovanovich, M.M. (1998). Conduction and thermal contact resistances (Conductances). In: *Handbook of Heat Transfer* (ed. W.M. Rohsenow, J.P. Hartnett, and Y.I. Cho), New York: McGraw-Hill.

3 Kakac, S. and Yener, Y. (1993). *Heat Conduction, Taylor & Francis*. Washington, DC.

4 Holman, J.P. (2010). *Heat Transfer*. McGraw Hill.

5 Mills, A.F. (1992). *Heat Transfer*. CRC Press.

6 Incropera, F.P., DeWitt, D.P., Bergman, T.L., and Lavine, A.S. (2006). *Fundamentals of Heat and Mass Transfer*, 6e. Wiley.

7 Shah, R.K. and London, A.L. (1978). *Laminar Flow Forced Convection in Ducts*. New York: Academic Press.

8 de Paulo Nicolau, V. and Dadam, A.P. (2009 October-December). Numerical and experimental thermal analysis of a tunnel kiln used in ceramic production. *J. Braz. Soc. Mech. Sci. & Eng.* XXXI (4): 297.

9 Biswas, S. and Sarkar, D. (2020). Introduction to refractories for iron and steel making. Switzerland: Springer Nature. ISBN 9783030438067.